The Astrophysical Journal Letters, 740:L23 (5pp), 2011 October 10 doi:10.1088/2041-8205/740/1/L23

SOLAR CYCLE VARIATIONS IN THE ELEMENTAL ABUNDANCE OF HELIUM AND FRACTIONATION OF IRON IN THE FAST SOLAR WIND: INDICATORS OF AN EVOLVING ENERGETIC RELEASE OF MASS FROM THE LOWER SOLAR ATMOSPHERE

Scott W. McIntosh[1], Kandace K. Kiefer[1,2], Robert J. Leamon[3], Justin C. Kasper[4], and Michael L. Stevens[4]
[1] High Altitude Observatory, National Center for Atmospheric Research, Boulder, CO 80307, USA
[2] Department of Earth & Atmospheric Sciences, Purdue University, West Lafayette, IN 47906, USA
[3] Department of Physics, Montana State University, Bozeman, MT 59717, USA
[4] Harvard-Smithsonian Center for Astrophysics, Smithsonian Astrophysical Observatory, Cambridge, MA 02138, USA
Received 2011 August 16; accepted 2011 September 6; published 2011 September 21

ABSTRACT

We present and discuss the strong correspondence between evolution of the emission length scale in the lower transition region and in situ measurements of the fast solar wind composition during the most recent solar minimum. We combine recent analyses demonstrating the variance in the (supergranular) network emission length scale measured by the *Solar and Heliospheric Observatory* (and *STEREO*) with that of the helium abundance (from *Wind*) and the degree of iron fractionation in the solar wind (from the *Advanced Composition Explorer* and *Ulysses*). The net picture developing is one where a decrease in the helium abundance and the degree of iron fractionation (approaching values expected of the photosphere) in the fast wind indicate a significant change in the process loading material into the fast solar wind during the recent solar minimum. This result is compounded by a study of the helium abundance during the space age using the NASA OMNI database, which shows a slowly decaying amount of helium being driven into the heliosphere over the course of several solar cycles.

Key words: solar wind – Sun: chromosphere – Sun: corona – Sun: heliosphere – Sun: surface magnetism – Sun: transition region

Online-only material: color figures

1. INTRODUCTION

Decrypting the physical processes encoded in the compositional measurements of the solar wind is akin to the use of DNA analysis in modern forensic science or archaeology to piece together a picture of what happened to whom, by whom, when, and where. The streams of particles captured by the compliment of solar wind composition instruments in interplanetary space are a literal treasure trove of physical information about the plasma from the time that it was originally heated in the solar atmosphere through any interactions it had with other streams en route to the detector. The distribution of ion charge states, densities, speeds, and atomic abundances among other things measured by these instruments form the DNA of the outer solar atmosphere's energetic processes and provide a significant challenge to our understanding as we are limited, for now, to remote sensing its day-to-day behavior and subtle evolution over decades.

In this Letter we start an investigation into some of the compositional measurements performed through the long, and unanticipated, activity minimum between solar cycles 23 and 24 where the reduced magnetic activity of the star (e.g., Smith & Balogh 2008; Wang et al. 2009) has allowed us to study the most basic, or basal, of energetic processes occurring in the solar atmosphere and their impact on the heliospheric system (e.g., McComas et al. 2008; Gibson et al. 2009; Solomon et al. 2010; McDonald et al. 2010; Mewaldt et al. 2010). This investigation was motivated by results presented in two recent papers by McIntosh et al. (2011b) and Kasper et al. (2011), where their key results are pictorially combined in Figure 1.

McIntosh et al. (2011b) demonstrated a variance in the dominant scale length of emission in the low transition region (TR), the (supergranular) magnetic network through the cycle 23/24 minimum. It was proposed that the scale length change was driven by the network vertices (and boundaries to a lesser degree) of the TR network emission being more sparsely packed with magnetic flux elements. The magnetic network reflects the scale length over which mass and energy are transported into the quiescent solar atmosphere (quiet Sun and coronal hole plasma alike; McIntosh et al. 2007; McIntosh & De Pontieu 2009) and so it was anticipated that a reduction in the network scale, driven by a change in the underlying magnetism, would impact the amount, and possibly the temperature, of material being inserted into the corona and solar wind. During the time that the mean network scale dropped below the 1996 minimum value (indicated on the plot as a horizontal dashed line) Kasper et al. (2011) noted a profound drop in the helium abundance ($A_{\rm He}$; defined as 100 times the ratio of the measured alpha particle and proton densities; Aellig et al. 2001) of the fast solar wind measured by the *Wind* spacecraft below that of the previous solar minimum. Note that the slower wind streams show far more variance with the solar activity cycle as well as showing a drop in helium abundance between the 1996 and 2009 minima. Yermolaev (1996) identified a similar pattern of helium abundance variability in solar wind streams with different magnetic (and atmospheric, e.g., coronal hole versus coronal mass ejection, etc.) origins using Prognoz 7 observations. However, we choose to focus our thoughts on the fast wind abundance change, motivated by the relative simplicity of fast wind origins in coronal holes (e.g., McIntosh et al. 2010), and also because its composition was considered to be relatively invariant—invariant to a degree that such a distinct, large amplitude change is extremely curious.

The remainder of this Letter follows the premise discussed by Parker (1991), and later promoted by McIntosh et al. (2010, 2011a), that the fast solar wind is populated and accelerated

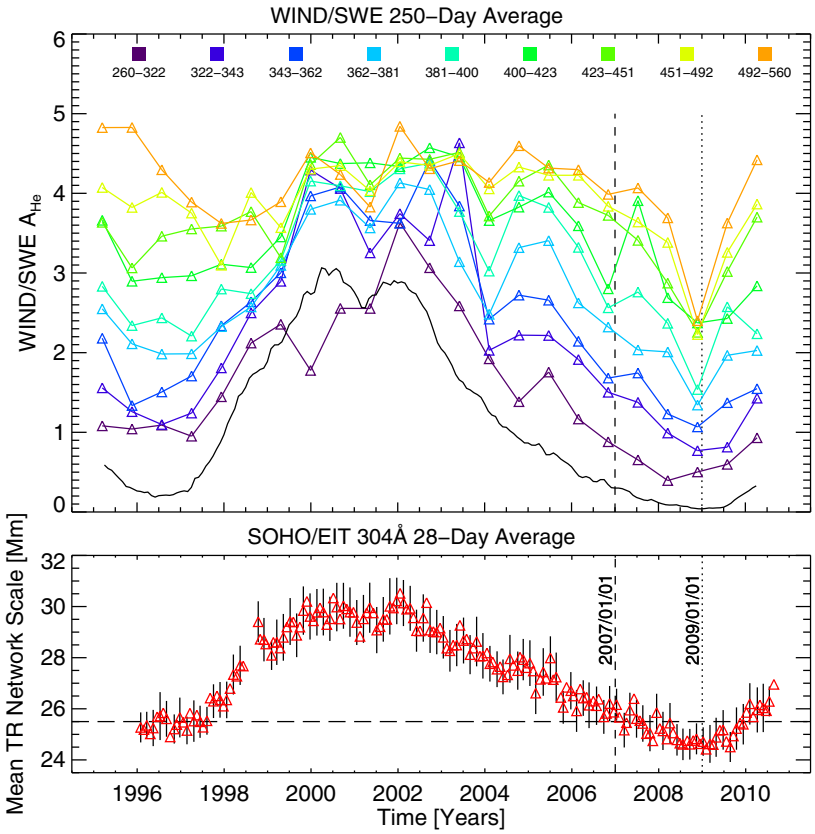

Figure 1. Combining the analysis of the *Wind* helium abundance (A_{He}) as a function of the solar wind speed in 250 day averages in the top panel (from Kasper et al. 2011) with the 28 day running average of the transition region (supergranular) network length scale from the *Solar and Heliospheric Observatory* (*SOHO*; McIntosh et al. 2011b). The solid black trace in the top panel shows the variation in the smoothed monthly sunspot number over the same time period. The dashed vertical line marks 2007 January 1 as an approximate date when the network scale falls below the mean value of the 1996 solar minimum. The time of minimum scale and helium abundance occur coincidently close to 2009 January 1.

(A color version of this figure is available in the online journal.)

by a tandem process. The first of these processes, heating the material out of the chromosphere to temperatures above 1 MK (De Pontieu et al. 2011; Martínez-Sykora et al. 2011), is necessary for the plasma to have enough thermal pressure to overcome gravity, accompanied by a second process that is able to accelerate the plasma to its final measured speed, e.g., low-frequency Alfvén waves (De Pontieu et al. 2007; McIntosh et al. 2011a). We have observed from Figure 1 that something has affected the deposition of helium in the solar wind during the last solar minimum—we presume that the coincident reduction in scale of the magnetic network has resulted in the abundance change observed in the fast solar wind. In the following sections we explore some of the compositional measurements obtained by the SWICS instrument on the *Ulysses* (Gloeckler et al. 1992) and the SWICS/SWIMS package on the *Advanced Composition Explorer* (*ACE*) (Gloeckler et al. 1998) to explore the composition of the fast solar wind during the recent solar minimum in and out of the ecliptic plane. To complete this preliminary analysis we perform the analysis of Kasper et al. (2011) on the NASA SPDF OMNI solar wind database, which provides alpha particle and proton densities back to the early 1970s, three complete solar cycles ago.

2. COMPOSITIONAL CHANGES

As we mentioned above, the composition of the solar wind likely reflects the physical conditions that the plasma meets from its original removal from the lower solar atmosphere until it finally finds itself on an open magnetic field line and travels outward into the heliosphere. Under our presumption above the fast solar wind composition then reflects the conditions set up by the rapid heating of the plasma from the chromosphere as illustrated recently in joint *Solar Dynamics Observatory* (*SDO*)/*Hinode* observations (De Pontieu et al. 2011). The slow solar wind, on the other hand, experiences some finite (but unknown) period of time in the closed corona of the quiet Sun or active regions before being able to escape. Therefore, its composition is likely to be far more complex and variable (Zurbuchen et al. 2002) as the phases of heating, cooling, ionization, and recombination are likely to play a role in setting up the mixture of ions and charge states that are observed in situ (see also the discussion and cartoon presented in De Pontieu et al. 2009). As we have said above, we will focus on the apparently simpler state of the fast solar wind.

In the following subsections we investigate the properties of ionic iron measured in the fast solar wind by the *Ulysses* and *ACE* spacecraft (see, e.g., von Steiger et al. 2010). We consider the degree of iron fractionation, D_{Fe}, which we define as the relative change in the measured iron-to-oxygen ratio (Fe/O) divided by the expected value of that ratio in the photosphere (e.g., the figures of Geiss et al. 1995), or 0.035 (Grevesse et al. 2007).

2.1. *Ulysses*/SWICS D_{Fe}

Figure 2 shows the difference between D_{Fe} in the fast and slow solar winds between the two solar "minimum" orbits of *Ulysses*, its first (left; 1992–1998) and third (right; 2004–2009), as a

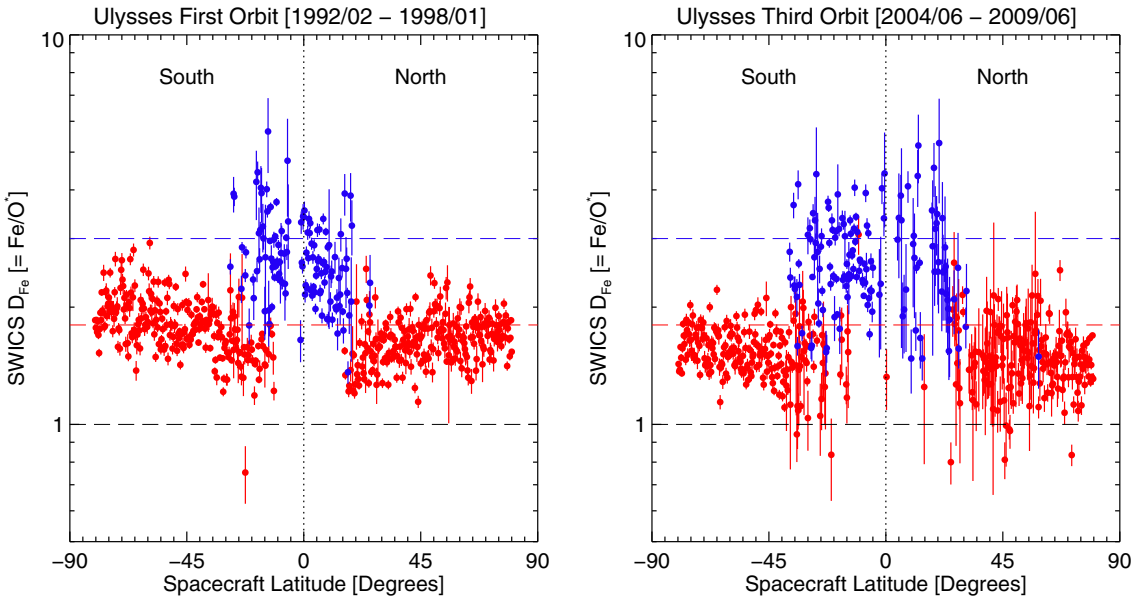

Figure 2. Comparing the degree of iron fractionation (D_{Fe}, the ratio of the iron and oxygen densities normalized by the expected photospheric value 0.035) measured over the first (left) and third (right) orbits of *Ulysses* by SWICS as a function of the heliographic latitude of the spacecraft. These orbits spanned the minima of cycle 22 into 23 and that of cycle 23 into 24, respectively. We have isolated the fast ($V_{SW} > 500$ km s^{-1}; red) and slow ($V_{SW} < 400$ km s^{-1}; blue) and plotted in 0°.5 bins of latitude. The horizontal dashed lines indicate values of $D_{Fe} = 1$ (black), $D_{Fe} = 1.8$ (red), and $D_{Fe} = 3$ (blue).

(A color version of this figure is available in the online journal.)

function of the spacecraft's heliospheric latitude.[5] The points and bars in the plot reflect the mean and standard deviations of D_{Fe} averaged over 0°.25 latitude bins for wind speeds less than 400 km s^{-1} (slow wind; blue) and greater than 500 km s^{-1} (fast wind; red). The horizontal dashed lines show values of $D_{Fe} = 1$ (black), $D_{Fe} = 1.8$ (red), and $D_{Fe} = 3$ (blue). The latter two are representative of typical fast and slow wind degrees of iron fractionation (see, e.g., Figure 2 of Geiss et al. 1995). Comparing the left and right panels of the figure we see that the measured values of D_{Fe} are systemically lower in the third orbit of *Ulysses* compared to that of its first.

We have repeated the analyses shown in Figure 2 using the technique of von Steiger et al. (2010) that discriminates between "fast" and "slow" wind based on charge state ratios rather than speed. However, the results are qualitatively (if not quantitatively) the same as those shown here, and we shall only further discuss solar wind speed as the discriminator.

2.2. *ACE*/SWICS D_{Fe} and Average Iron Charge

Figure 3 shows the variation of D_{Fe} in the top panel and the average iron charge state, $\langle Q_{Fe} \rangle$, in the bottom panel over the entire *ACE* mission—unfortunately *ACE* did not sample the 1996 minimum, but we will use the observations to look for systematic changes in the declining phase of cycle 23 and the 2009 solar minimum in the ecliptic plane. Isolating the fast and slow wind streams in the same way as above (red for $V_{SW} > 500$ km s^{-1}; blue for $V_{SW} < 400$ km s^{-1}) and averaging the measurements of Fe/O (and $\langle Q_{Fe} \rangle$) over a day we see the systemic difference between fast and slow wind values of D_{Fe} where we have again drawn the dashed lines indicating values of 1, 1.8, and 3. The fast and slow winds show a systematically offset slow decline in D_{Fe} in the declining phase of cycle 23, with the latter reaching values of the order of 1.3 before rapidly increasing again at the start of 2009. The lower panel of Figure 3 shows the variance of $\langle Q_{Fe} \rangle$ for fast and slow wind streams through the cycle 23 solar maximum, through the declining phase, and into the deep solar minimum of 2009. The values of $\langle Q_{Fe} \rangle$ in the fast and slow winds drop from 10 in 2005 to a value of ~8.5 for the fast wind and ~9 for the slow wind at the start of 2009 before increasing rapidly. Note the dashed line drawn for Fe^{9+} (or "Fe X" in spectroscopic notation) and that the right-hand scale of the lower panel shows an approximate value for the temperature at which that charge state reaches maximum population, roughly $T \sim 10^4(Q+1)^2$ K. So, not only does the value of D_{Fe} drop during the 2009 solar minimum to values consistent with the measurements of *Ulysses* out of the ecliptic plane, but the inferred temperature of the plasma (under equilibrium conditions) appears to be systematically lower into the period where the network scale reached its minimum.

3. STEADY DECAY OVER MANY MINIMA?

In Figure 4, we show the results of performing the velocity-discriminating A_{He} analysis of Kasper et al. (2011) on the NASA SPDF OMNI solar wind database record of the alpha/proton ratio. Separating the fast (>500 km s^{-1}; red) and slow (<400 km s^{-1}; blue) wind streams and performing a 50 day running average we can compare the variation in the solar wind A_{He} with magnetic activity back to 1970, noting that from 1994 onward many of the measurements come from *Wind*, like those in Figure 1. Like Figure 1 there is stronger modulation in A_{He} in the slow wind, but it is still present in the fast wind, which also shows a systematically slower decay in the descending phase of the cycles. Over the entire time period, and particularly from 1980, the values of A_{He} inferred show a steady decline with the reduction in large-scale solar activity. While this plot is striking in its trends and variance, it must be considered carefully as it is a unique single record composed of measurements from many spacecraft and, as such, is dependent on the intercalibration of

[5] Orbit one covered the declining phase of cycle 22 and ascent of cycle 23 while orbit three sampled the declining phase of cycle 23 into and through the 2009 minimum.

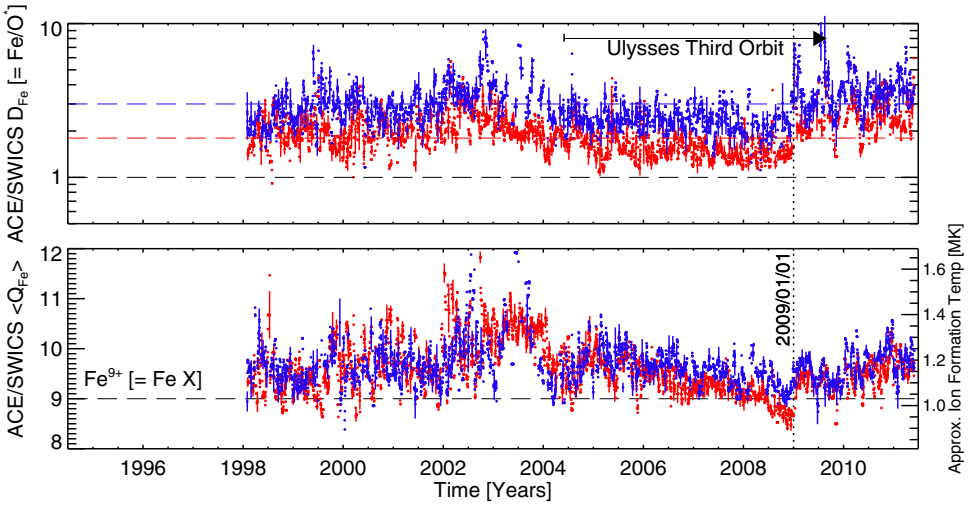

Figure 3. Comparing the daily averages in the degree of iron fractionation ($D_{\rm Fe}$; top) and the average iron charge state ($\langle Q_{\rm Fe}\rangle$; bottom) in the fast ($V_{\rm SW} > 500$ km s^{-1}; red) and slow winds ($V_{\rm SW} < 400$ km s^{-1}; blue) through the 2009 solar minimum as measured by *ACE*/SWICS in the ecliptic plane—2009 January 1 is indicated by a vertical dotted line. In the upper panel the horizontal dashed lines indicate values of $D_{\rm Fe} = 1$ (black), $D_{\rm Fe} = 1.8$ (red), and $D_{\rm Fe} = 3$ (blue), and an arrow is drawn to illustrate the duration of the third orbit of *Ulysses* through the declining phase of cycle 23. In the bottom panel a horizontal dashed line is drawn at $\langle Q_{\rm Fe}\rangle = 9$ for the reference of the reader.

(A color version of this figure is available in the online journal.)

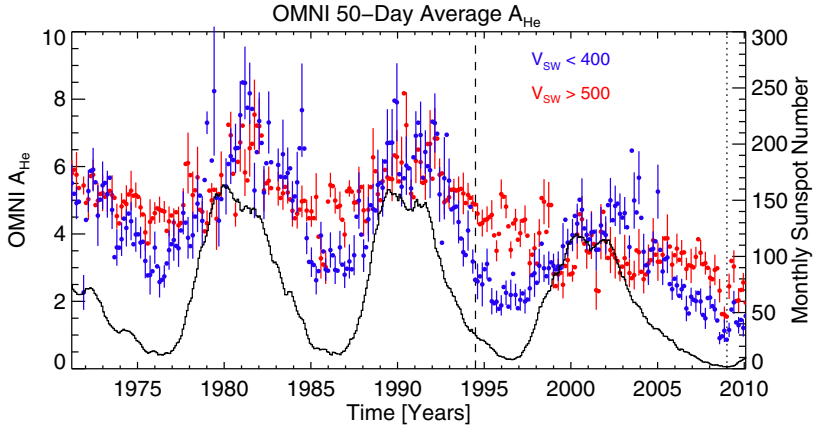

Figure 4. Using the OMNI database to extend 50 day averages of $A_{\rm He}$ shown in Figure 1 back through other cycles for fast ($V_{\rm SW} > 500$ km s^{-1}; red) and slow ($V_{\rm SW} < 400$ km s^{-1}; blue) winds. Again, 2009 January 1 is indicated by a vertical dotted line while 2004 June 1 is indicated by a vertical dashed line to mark the start of the *Wind* measurements shown in Figure 1. The solid black trace shows the variation in the smoothed monthly sunspot number over the time period.

(A color version of this figure is available in the online journal.)

those measurements, but since there is no obvious sign of discontinuous jumps in the record over with a range of averaging windows it would appear that the OMNI alpha/proton record is of high internal consistency. The measure of this variance is the continued monitoring of these values in the ecliptic plane into and through the ascending phase of cycle 24.

4. DISCUSSION

We have observed a significant decrease in the helium abundance in the fast solar wind occuring in the recently past solar minimum. In addition, we have observed that the degree of iron fractionation measured by the SWICS instruments on the *Ulysses* and *ACE* spacecraft have receded from their typical value of ∼2 and have approached values nearer unity over the same period in time. The latter spacecraft has also allowed us to investigate the variation in the mean charge state of iron and a clear, steady drop is seen in the fast wind over the declining phase of solar cycle 23 hitting a minimum value at the start of 2009.

On the Sun at this time, the (supergranular) network length scale reached a minimum. That length scale, mediated by the distribution of the small-scale photospheric magnetic field, dictates the flow of mass and energy into the quiescent solar atmosphere. These observational results are consistent with a situation where the decay in the length scale, driven by the persistent diffusion of the magnetic field to smaller length scales (McIntosh et al. 2011b) has affected the amount of energy supplied to heat the fast wind plasma at its roots, dropping its particle density (e.g., McComas et al. 2008) and mean iron charge state. The high first ionization potential (FIP) of helium almost certainly ensures its strong sensitivity to a small change in the plasma heating present in the quiescent solar network. Furthermore, this is also consistent with the reduced degree of iron fractionation measured in, and out of, the ecliptic plane at the same time. While the physical process responsible for the "FIP effect" in fast or slow winds is, as yet, undetermined it is clear that the plasma is being less "aggressively" heated at its roots—and so, for the fast wind at least, the plasma heating process in the lower solar atmosphere must play an essential

role in establishing the degree of fractionation observed (Geiss et al. 1995). It is likely that the excessive low-FIP element fractionation of the slow solar wind is complicated further by the circulation of heated and cooling material (see the cartoon of De Pontieu et al. 2009) and is far beyond the scope of this Letter in complexity, but is an interesting item of further study. Similarly, it is not yet clear how the discrete heating events we discuss here scale in magnitude or number with the complexity (number of small-scale same polarity flux bundles) of the magnetic network vertices, suffice it to say, that it would appear to play some prominent role in the initial (heating) phase of the mass cycle and is being reflected directly in the particulate emissions of coronal holes rather than those of the magnetically closed quiet Sun and active regions.

The fact that there is still a solar wind at speeds greater than 500 km s^{-1} is likely further evidence in support of the notion that the fast solar wind is a result of a two-stage process, the first to heat the plasma low in the solar atmosphere, combined with a second phase acting away from the solar surface to accelerate the wind to its final measured speed as was speculated by Parker (1991) and more recently revisited by McIntosh et al. (2010, 2011a). This result is accentuated by a study of the helium abundance during the space age using the NASA OMNI database, which clearly shows a slowly decaying amount of helium being driven into the heliosphere over the course of the several solar cycles indicative of a slowly decaying background magnetic field and the resulting reduction in energy heat supply and the resulting mass release.

5. INTERPRETATION

We propose that the observed decreases in $A_{\rm He}$ and the $D_{\rm Fe}$ (approaching values expected of the photosphere) in the fast wind indicate a significant change in the process loading material into the fast solar wind during the recent solar minimum. The mean fast solar wind speed shows a small decrease between the two minima (McComas et al. 2008), but the abundance change observed is profound—indicating to us that the amount of energy deposited into the plasma has changed dramatically. We believe that this is justification for our premise that the process heating the fast solar wind plasma and that which subsequently accelerates it into interplanetary space are, at best, loosely coupled (having different length scales of dissipation) even though they are rooted in the (prevalent) network length scale. As we have stated above the mechanism heating the plasma in unipolar flux concentrations such as those forming the network vertices is still not clear (De Pontieu et al. 2011), but we can speculate on why the fast wind $A_{\rm He}$, $D_{\rm Fe}$, and $\langle Q_{\rm Fe}\rangle$ changed in the last solar minimum and may be continuing to reduce from minimum to minimum over recent decades.

Based on the primary inference of McIntosh et al. (2011b), the ongoing diffusion of the quiet-Sun magnetism to smaller length scales reduced the number (and possibly also the strength) of the magnetic elements (e.g., *G*-band bright points) in the network vertices. Given that the strongest heating events predominantly occur in the proximity of these unipolar magnetic structures (De Pontieu et al. 2009), it would seem sensible to infer that the heating rate depends critically on the arrangement of the discrete flux elements of the vertex and not only on their strength.[6] Helium, having the highest FIP will feel this (subtle) change in plasma heating most and iron, given that it is rapidly ionized, will have less time to establish strong fractionation and a lower charge state. Therefore, we believe that reduced plasma heating strength (and/or frequency) in the lower solar atmosphere—driven by the diffusion of the field—reduced the "complexity" of the network vertices and this modified the plasma heating, which then led to the changes in fast solar wind composition. We note that it is a different challenge to identify what is happening to the underlying magnetism at the root of the declining helium abundance over the past several solar cycles.

[6] It is not clear how the heating event frequency and strength scale with the number of flux elements or their strength, but is an important avenue to be tested observationally and numerically (e.g., Martínez-Sykora et al. 2011) in the near future.

S.W.M. is supported by NSF ATM-0541567 (ATM-0925177), NASA grants NNG06GC89G, NNX08AL22G, and NNX08AH45G. K^3 visited HAO in the summer of 2011 supported by the NSF Research Experience for Undergraduates (REU) program—we greatly appreciate the organization and commitment of the CU/LASP REU program administration group. In addition, we thank Joe Gurman for valuable comments, the *Ulysses*/SWICS and *ACE*/SWICS instrument teams for the effort taken to distribute and document the ion composition they serve to the community, and likewise to the OMNI database staff for their continued effort to preserve an essential physical record. NCAR is sponsored by the National Science Foundation.

REFERENCES

Aellig, M. R., Lazarus, A. J., & Steinberg, J. T. 2001, Geophys. Res. Lett., 28, 2767
De Pontieu, B., McIntosh, S. W., Carlsson, M., et al. 2007, Science, 318, 1574
De Pontieu, B., McIntosh, S. W., Carlsson, M., et al. 2011, Science, 331, 55
De Pontieu, B., McIntosh, S. W., Hansteen, V. H., & Schrijver, C. J. 2009, ApJ, 701, L1
Geiss, J., Gloeckler, G., von Steiger, R., et al. 1995, Science, 268, 1005
Gibson, S. E., Kozyra, J. U., de Toma, G., et al. 2009, J. Geophys. Res. (Space Phys.), 114, 9105
Gloeckler, G., Cain, J., Ipavich, F. M., et al. 1998, Space Sci. Rev., 86, 497
Gloeckler, G., Geiss, J., Balsiger, H., et al. 1992, A&AS, 92, 267
Grevesse, N., Asplund, M., & Sauval, A. J. 2007, Space Sci. Rev., 130, 105
Kasper, J. C., et al. 2011, ApJ, in press
Martínez-Sykora, J., Hansteen, V., & Moreno-Insertis, F. 2011, ApJ, 736, 9
McComas, D. J., Ebert, R. W., Elliott, H. A., et al. 2008, Geophys. Res. Lett., 35, 18103
McDonald, F. B., Webber, W. R., & Reames, D. V. 2010, Geophys. Res. Lett., 37, 18101
McIntosh, S. W., Davey, A. R., Hassler, D. M., et al. 2007, ApJ, 654, 650
McIntosh, S. W., & De Pontieu, B. 2009, ApJ, 707, 524
McIntosh, S. W., De Pontieu, B., Carlsson, M., et al. 2011a, Nature, 475, 477
McIntosh, S. W., Leamon, R. J., & De Pontieu, B. 2010, ApJ, 727, 7
McIntosh, S. W., Leamon, R. J., Hock, R. A., Rast, M. P., & Ulrich, R. K. 2011b, ApJ, 730, L3
Mewaldt, R. A., Davis, A. J., Lave, K. A., et al. 2010, ApJ, 723, L1
Parker, E. N. 1991, ApJ, 372, 719
Smith, E. J., & Balogh, A. 2008, Geophys. Res. Lett., 35, 22103
Solomon, S. C., Woods, T. N., Didkovsky, L. V., Emmert, J. T., & Qian, L. 2010, Geophys. Res. Lett., 37, 16103
von Steiger, R., Zurbuchen, T. H., & McComas, D. J. 2010, Geophys. Res. Lett., 37, 22101
Wang, Y.-M., Robbrecht, E., & Sheeley, N. R., Jr. 2009, ApJ, 707, 1372
Yermolaev, Y. I. 1996, in AIP Conf. Proc. 382, Eighth Int. Solar Wind Conf., ed. D. Winterhalter et al. (Melville, NY: AIP), 269
Zurbuchen, T. H., Fisk, L. A., Gloeckler, G., & von Steiger, R. 2002, Geophys. Res. Lett., 29, 1352